Atmospheric Environment 85 (2014) 169–178

Contents lists available at ScienceDirect

Atmospheric Environment

journal homepage: www.elsevier.com/locate/atmosenv

Response of the ozone column over Europe to the 2011 Arctic ozone depletion event according to ground-based observations and assessment of the consequent variations in surface UV irradiance

Boyan H. Petkov [a,b,*], Vito Vitale [a], Claudio Tomasi [a], Anna Maria Siani [c], Gunther Seckmeyer [d], Ann R. Webb [e], Andrew R.D. Smedley [e], Giuseppe Rocco Casale [c], Rolf Werner [f], Christian Lanconelli [a], Mauro Mazzola [a], Angelo Lupi [a], Maurizio Busetto [a], Henri Diémoz [g], Florence Goutail [h], Ulf Köhler [i], Bogdana D. Mendeva [f], Weine Josefsson [j], David Moore [k], María López Bartolomé [l], Juan Ramón Moreta González [l], Oliver Mišaga [m], Arne Dahlback [n], Zoltán Tóth [o], Saji Varghese [p], Hugo De Backer [q], René Stübi [r], Karel Vaníček [s]

[a] Institute of Atmospheric Sciences and Climate (ISAC), Italian National Research Council (CNR), Via Gobetti 101, I-40129 Bologna, Italy
[b] International Centre for Theoretical Physics (ICTP), Strada Costiera 11, I-34014 Trieste, Italy
[c] Sapienza University, Rome, Piazzale Aldo Moro 5, 00185 Rome, Italy
[d] Institute of Meteorology and Climatology, Leibniz University of Hannover, Hannover, Germany
[e] School of Earth, Atmospheric and Environmental Sciences, University of Manchester, Oxford Road, Manchester M13 9PL, UK
[f] Space Research and Technology Institute, Bulgarian Academy of Sciences, Stara Zagora Department, Bulgaria
[g] Arpa Valle d'Aosta, Loc. Grande Charrière 44, 11020 Saint-Christophe (AO), Italy
[h] LATMOS, CNRS – Université Versailles St Quentin, 11 Boulevard d'Alembert, 78280 Guyancourt, France
[i] Meteorological Observatory Hohenpeissenberg, Albin Schwaiger Weg 10, 82383 Hohenpeissenberg, Germany
[j] Swedish Meteorological and Hydrological Institute, SE-601 76 Norrköping, Sweden
[k] United Kingdom Meteorological Office, FitzRoy Road, Exeter, Devon EX1 3PB, United Kingdom
[l] Special Networks and Atmosphere Watch Service, State Meteorological Agency from Spain (AEMET), c/Leonardo Prieto 8, 28040 Madrid, Spain
[m] Centre of Aerology and Solar Radiation, Slovak Hydrometeorological Institute, 058 01 Poprad-Gánovce, Slovakia
[n] University of Oslo, Department of Physics, P. O. Box 1048, N-0316 Oslo, Norway
[o] WMO Regional Centre for Solar Radiation Atmospheric Physics and Measurement Techniques Division Hungarian Meteorological Service, Budapest, Hungary
[p] Valentia Geophysical and Meteorological Observatory, Irish Meteorological Service (Met Éireann) Caherciveen, Co. Kerry, Ireland
[q] Royal Meteorological Institute of Belgium, Ringlaan 3, B-1180 Brussels, Belgium
[r] Federal Office of Meteorology and Climatology, MeteoSwiss, Ch. de l'Aérologie 1, CH-1530 Payerne, Switzerland
[s] Solar and Ozone Observatory, Czech Hydrometeorological Institute, Hvězdárna 456, 500 08 Hradec Králové 8, Czech Republic

HIGHLIGHTS

- We examine the effect of Arctic ozone depletions on the ozone column over West Europe.
- The measurements of ozone column performed at 34 European stations have been analysed.
- The daily ozone column distributions over Europe were reconstructed and studied.
- Strong impact of the 2011 Arctic ozone depletion on mid-latitude ozone was ascertained.
- The effect of the 2011 ozone depletion on surface UV over Europe has been analysed.

ARTICLE INFO

Article history:
Received 28 April 2013
Received in revised form
1 December 2013
Accepted 4 December 2013

ABSTRACT

The strong ozone depletion event that occurred in Arctic during spring 2011 was found to cause appreciable reduction in the ozone column (OC) in Europe, even at lower latitudes. The features of this episode have been analysed using the data recorded at 34 ground-based stations located in the European area and compared with the similar events in 2000 and 2005. The results provided evidence that OC as far

* Corresponding author. Institute of Atmospheric Sciences and Climate (ISAC), Italian National Research Council (CNR), Via Gobetti 101, I-40129 Bologna, Italy.
E-mail address: b.petkov@isac.cnr.it (B.H. Petkov).

http://dx.doi.org/10.1016/j.atmosenv.2013.12.005

Keywords:
Ozone depletion
Arctic ozone
Solar UV irradiance
Ozone impact on surface UV

south as 40°N latitude was considerably influenced by the Arctic ozone loss in spring 2011. The reduction of OC at the northernmost sites was about 40% with respect to the mean value calculated over the previous six-year period, while a similar decrease at the southern extreme ranged between 15 and 18%, and were delayed by nearly two weeks compared to the Arctic region. The ozone distributions reconstructed for the West Europe sector show that the decline of OC lasted from late March to late April 2011. The echo of the Arctic ozone depletion on mid-latitude UV irradiance has been analysed trough model computations that show an increase of the midday erythemal dose by 3–4 SED (1 SED = 100 J m^{-2}) that was slightly higher than at polar regions. On the other hand it was assessed that the biosystems in the northernmost regions were a subject of about 4 times higher UV stress than those at mid-latitudes. Despite indications of an OC recovery, the event examined here shows that the issue of ozone depletion episodes cannot be belittled.

1. Introduction

Ozone plays an important role in the Earth's energy balance through its important effects on radiative processes, interacting with both solar and infrared terrestrial radiation (Brasseur and Solomon, 2005; WMO, 2007). It is also vitally important to life because of its strong absorption of biologically harmful solar ultraviolet (UV) radiation (Lucas et al., 2006). Observations performed during recent decades indicate that atmospheric ozone was subject to a variety of anomalies on different spatial and temporal scales. So-called "ozone mini-holes" (Siani et al., 2002; Mangold et al., 2009; Werner et al., 2009) are characterized by significant ozone decreases lasting 1–3 days over limited geographical regions and are associated with synoptic weather systems (Dobson et al., 1929). In contrast the Antarctic ozone depletion discovered in the middle of the 1980s (Farman et al., 1985), covers an area of continental extent and is more persistent. The reduction in ozone observed at middle latitudes since the end of 1970s (WMO, 1998, Antón et al., 2011) and the severe Antarctic ozone depletion, led to the Montreal Protocol on Substances that Deplete the Ozone Layer (http://www.unep.org/ozone) and its subsequent amendments and adjustments. However, despite expectations that ozone is beginning to return to pre-1980s levels (WMO, 2010; Antón et al., 2011; Zerefos et al., 2012), knowledge of its complex interactions with the processes regulating the climate is still limited. Although the ozone destruction mechanisms are quite well understood, several unexpected ozone depletions have sporadically occurred during the last two decades over the Arctic region (WMO, 2007; Manney et al., 2011), due to particular meteorological conditions.

According to current understanding, the reduction of the ozone column (OC) in Antarctica is a result of chemical destruction by photolytic reactions taking place in the very stable polar vortex, which creates favourable conditions for ozone depletion (Molina and Rowland, 1974; Crutzen and Arnold, 1986). Conversely, the vortex over the Arctic is less stable and frequently disturbed by Rossby waves (Hauchecorne et al., 2002), inhibiting the chemical processes of ozone loss. In addition, the Brewer-Dobson circulation, more intensive in the North hemisphere, maintains comparatively high ozone concentration over the northern polar regions (WMO, 2010). However, the cold vortices observed in the 1995/1996, 1996/1997, 1999/2000, 2004/2005 and 2010/2011 winters contributed to OC depletion occurrences during the winter–spring months (Hauchecorne et al., 2002; Koch et al., 2004; WMO, 2007; Rösevall et al., 2008; Arnone et al., 2012). The last of these occurrences, caused by an extremely cold and stable polar vortex conducive to the chemical ozone loss, was found to be comparable in intensity with the corresponding Antarctic events (Manney et al., 2011). The features of the Arctic ozone loss within the vortex have been studied in detail since the mid-nineties (e.g. the MATCH campaigns: von der Gathen et al., 1995; Rex and von der Gathen, 2007; Thompson et al., 2011).

To complement the satellite stratospheric research, this paper analyses the response of the OC over Western Europe to the 2011 Arctic depletion event. The measurements, performed by various instruments at numerous stations located along European meridians between about 40°N and 80°N parallels, were analysed to characterize the variations at mid-latitudes, comparing them with

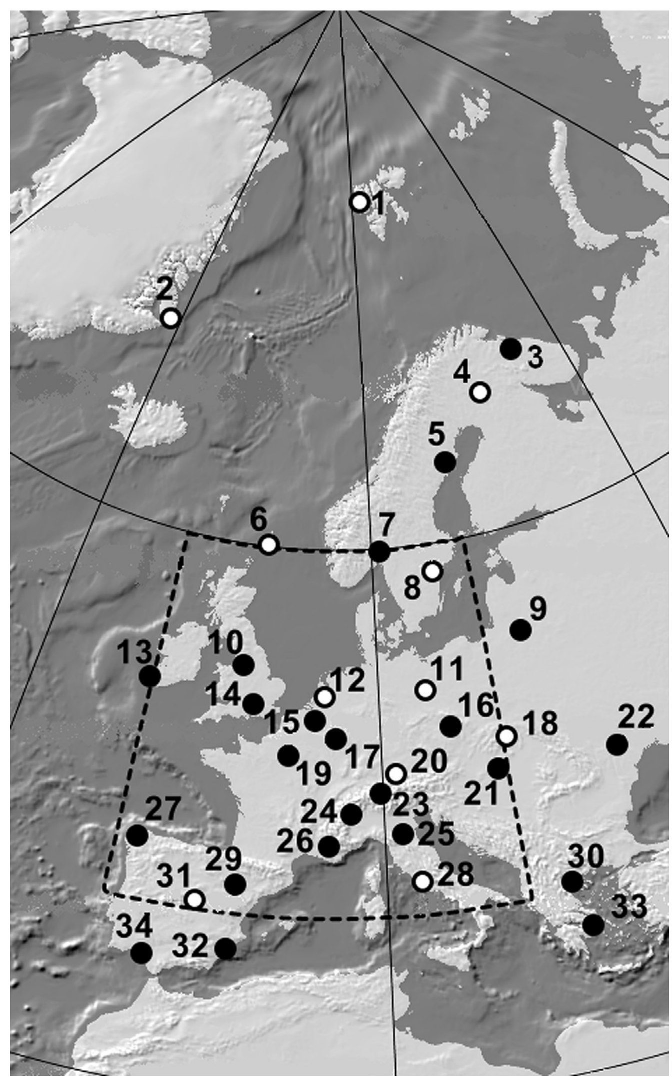

Fig. 1. Map of the stations, whose data are used in the present analysis. The numbers identifying the stations are the same given in Table 1. The stations considered in Section 3 are represented by white circles. The sector limited by the longitude and latitude dashed isopleths was the subject of the analysis presented in Section 4.

Table 1
List of the stations considered in the present analysis with the corresponding coordinates and measurement period. The major part of the data were downloaded from the web site of World Ozone and Ultraviolet Data Centre (WOUDC, 2012); the stations taken part of this data-set are labelled by superscript "W". The stations equipped with SAOZ spectrometer (Pommereau and Goutail, 1988) for which the data were taken from SAOZ (2012) web site are labelled by superscript "Z". In addition, two narrow-band filter radiometers UV-RAD (Petkov et al., 2012, 2013) have been also included.

N	Station, country, instrument	Latitude	Longitude	Period
1	Ny-Ålesund[Z], Norway, UV-RAD[a)], SAOZ	78°56′ N	11°56′ E	2007–2011
2	Scoresbysund[W], Greenland, SAOZ	70°29′ N	21°59′ W	2000–2011
3	Murmansk[W], Russia, Filter M-124 220.	68°58′ N	33°04′ E	2000–2009
4	Sodankyla[Z], Finland, SAOZ	67°25′ N	26°35′ E	2000–2011
5	Vindeln[W], Sweden, Brewer MKII 006.	64°14′ N	19°46′ E	2000–2011
6	Lerwick[W], UK, Dobson Beck 032, 041	60°08′ N	01°11′ W	2000–2011
7	Oslo[W], Norway, Brewer MKV 042	59°56′ N	10°46′ E	2000–2011
8	Norrköping[W], Sweden, Brewer MKIII 128	58°35′ N	16°09′ E	2000–2011
9	Kaunas[W], Lithuania, Filter M-124 459, 463	54°31′ N	23°32′ E	2000–2011
10	Manchester[W], UK, Brewer MKIII 172	53°29′ N	02°14′ W	2000–2011
11	Lindenberg[W], Germany, Brewer MKIV 030, MKII 078	52°13′ N	14°07′ E	2000–2011
12	De Bilt[W], Netherlands, Brewer MKIII 100, 189	52°06′ N	05°11′ E	2000–2011
13	Valentia Observatory[W], Ireland, Brewer MKIV 088	51°56′ N	10°15′ W	2000–2011
14	Reading[W], UK, Brewer MKIV 075, MKII 126	51°27′ N	00°56′ W	2002–2011
15	Uccle[W], Belgium, Brewer MKII 016, MKIII 178	50°48′ N	04°21′ E	2000–2011
16	Hradec Kralove[W], Czech Republic, Brewer MKIII 184	50°06′ N	15°50′ E	2000–2011
17	Diekirch[W], Luxembourg, Microtops II 3012, 5375	49°52′ N	06°10′ E	2001–2011
18	Poprad-Ganovce[W], Slovakia, Brewer MKIV 097	49°02′ N	20°19′ E	2000–2011
19	Paris[Z], France, SAOZ	48°52′ N	02°19′ E	2006–2011
20	Hohenpeissenberg[W], Germany, Brewer.MKII.010	47°48′ N	11°01′ E	2000–2011
21	Budapest-Lorinc[W], Hungary, Brewer MKII 152	47°26′ N	19°11′ E	2000–2011
22	Chişinău[W], Moldova, Microtops II 7351	47°00′ N	28°49′ E	2003–2011
23	Arosa[W], Switzerland, Brewer MKII 040	46°47′ N	09°41′ E	2000–2011
24	Aosta[W], Italy, Brewer MKIV 066	45°42′ N	07°22′ E	2007–2011
25	Bologna, Italy, UV-RAD	44°31′ N	11°20′ E	2006–2011
26	Haute Provence[W], France, SAOZ, Dobson Beck 085	43°56′ N	05°42′ E	2000–2011
27	La Coruña[W], Spain, Brewer MKIV 151, 070	43°20′ N	08°28′ W	2000–2011
28	Rome University[W], Italy, Brewer MKIV 067	41°54′ N	12°31′ E	2000–2011
29	Zaragoza[W], Spain, Brewer MKIV 166	41°38′ N	00°55′ W	2000–2011
30	Thessaloniki[W], Greece, Brewer MKII 005	40°31′ N	22°58′ E	2000–2010
31	Madrid[W], Spain, Brewer MKIV 070	40°27′ N	03°43′ W	2000–2011
32	Murcia[W], Spain, Brewer MKIV 117	38°00′ N	01°10′ W	2000–2011
33	Athens[W], Greece, Dobson Beck 118	37°59′ N	23°45′ E	2000–2011
34	El Arenosillo[W], Spain, Brewer MKIII 150, Dobson Beck 120	37°06′ N	06°44′ W	2000–2011

[a] Data recorded in 2010 and 2011 only.

the corresponding 2000 and 2005 OC variations caused by similar depletions. In addition, the response of surface UV irradiance to such events has been analysed by use of a radiative transfer model.

2. Data-set

To characterise the effects caused by the Arctic ozone depletion that occurred in spring 2011 we analysed data provided by 34 ground-based stations located from the Svalbard Archipelago to the Mediterranean over the area shown in Fig. 1. Table 1 gives the geographical coordinates of all the stations, the instrument model employed at each site, and the period for which data were available. Hereinafter the name of each station will be followed in the text by a bracket containing the letter "*S*" (meaning "station") followed by the identification number given in both Table 1, and Fig. 1.

As a part of a global network, the instruments used in the present study were subject to regular calibration procedures to assure high quality data. Except for periodic checks and tests (monthly, weekly and daily), the operating Brewer spectrophotometers are biennially calibrated by comparing them with the reference to the IOS Inc. (International Ozone Service, http://www.io3.ca/Calibrations) instrument, the World triad of instruments in Toronto, or the European triad in Izaña. In some stations with Brewer MKIII instruments the ozone calibration is performed by Kipp and Zonen Inc. (www.kippzonen.com). The ozone data extracted by the World Ozone and Ultraviolet Data Centre database were widely used in the recent years for satellite validations (Balis et al., 2007; Fioletov et al., 2008; Ialongo et al., 2008; Hendrick et al., 2011). The accuracy of well-maintained Dobson and Brewer instruments were estimated to be 0.5% and 0.15%, respectively, and the differences with respect to satellite products were found to vary from 0.6 to 2.6% for Brewers and Dobsons and between 1.5 and 3.5% for filter instruments (WMO, 2010).

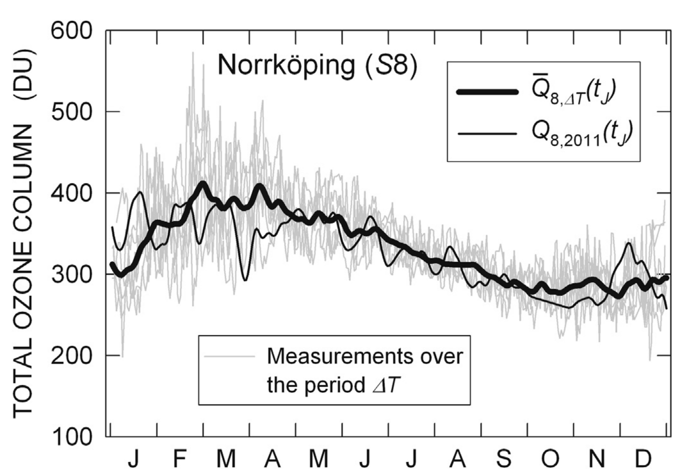

Fig. 2. Time-patterns of daily OC (in Dobson Units, DU), as obtained through the averaging and smoothing procedures adopted to evaluate the variables $\overline{Q}_{S,\Delta T}(t_J)$ and $Q_{S,Y}(t_J)$ for the data-set recorded at the Norrköping (*S*8) station in year $Y = 2011$. The mean ozone variation curve $\overline{Q}_{8,\Delta T}(t_J)$ was obtained by averaging and smoothing the annual time-patterns $Q'_{S,Y}(t_J)$ (thin grey curves). Parameter $Q_{8,2011}(t_J)$ describes the time-patterns of OC measured in 2011 and smoothed after filling all the gaps through a linear interpolation procedure in time.

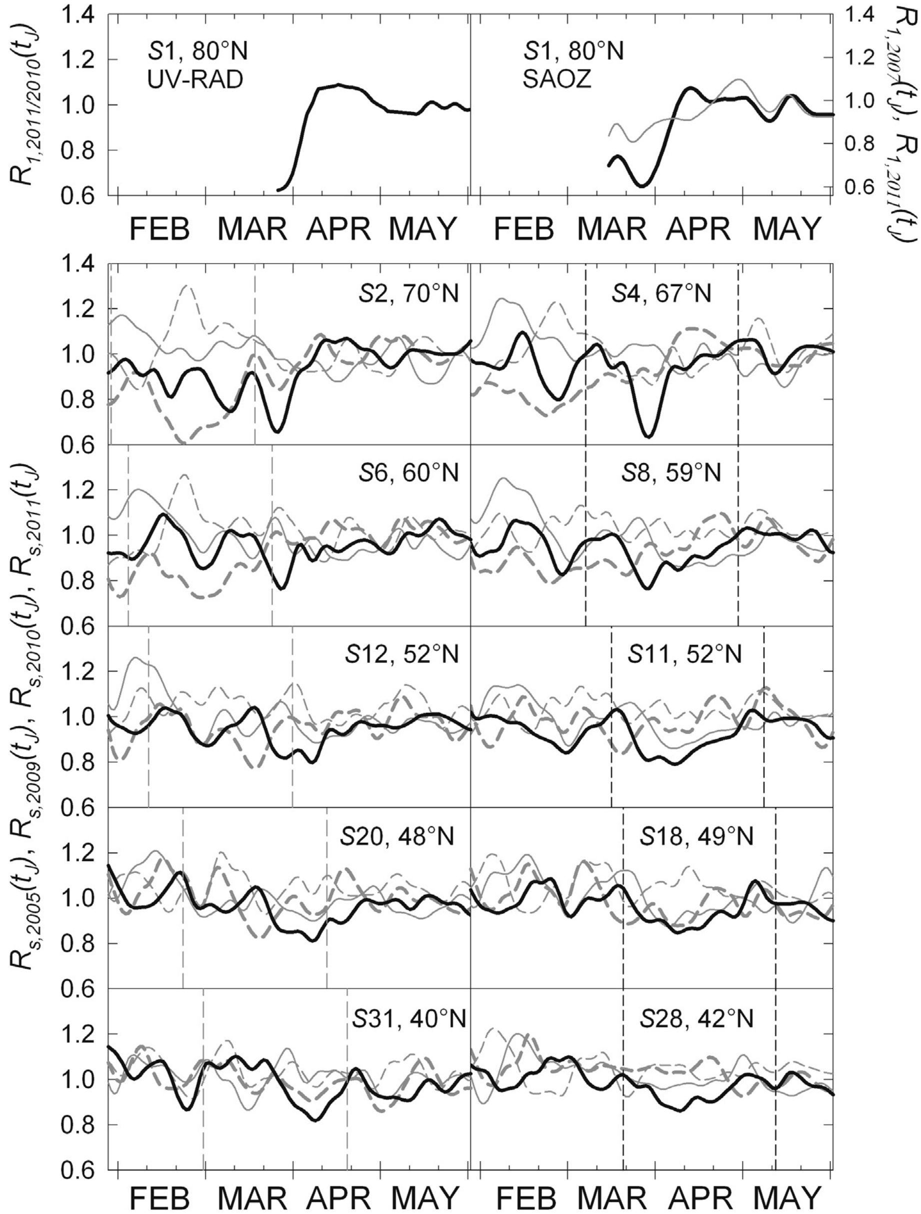

Fig. 3. Variations in OC at the selected stations, labelled in Fig. 1 with white circles, during the February–May period of different years and determined by the ratios evaluated in terms of Eq. (1). Upper part shows the ozone changes recorded at Ny-Ålesund (*S*1) using the UV-RAD (left) and SAOZ (right) instruments, respectively given by ratios $R_{1,2011/2010}(t_J)$ and $R_{1,2011}(t_J)$ (thick curves), and $R_{1,2007}(t_J)$ (grey curve). The lower part shows the ozone variations measured in 2011 (thick black curves) together with the corresponding variations measured in years 2005 (thick dashed grey curves), 2009 (thin grey curves), and 2010 (thin dashed grey curves). The stations are indicated by the letter "*S*" followed by the corresponding identification numbers given in Table 1. The vertical dashed lines define the periods found to present similar features of the variations and discussed in Section 3.3 for the years 2005 (left) and 2011 (right).

3. Latitudinal characteristics of the ozone column variations during spring 2011

The results obtained from the data-sets recorded at 11 European stations (Fig. 1) were used to examine the main OC variations along the meridian during spring 2011. The stations were chosen to attain nearly regularly spaced observational points ranging between about 80°N and 40°N latitudes, following two different trajectories, both starting from Ny-Ålesund (*S*1) and ending at Madrid (*S*31) and Rome (*S*28), respectively.

3.1. Parameterization of the ozone column variations

To correctly determine the meridional characteristics of the OC variations during spring 2011, they were compared at each selected station with the corresponding reference behaviour found by computing the mean ozone time-patterns in preceding years chosen to represent the typical OC behaviour. In the previous decade, the years 2000 and 2005 were characterized by deep ozone depletions over the polar regions (Koch et al., 2004; Von Hobe et al., 2006; Rösevall et al., 2008; Manney et al., 2011), while the sudden stratospheric warming occurred in late February 2008 caused a significant reduction of OC over North Europe (Flury et al., 2009). Bearing in mind these events, the period ΔT taken to assess the reference behaviour of OC in the study area was determined by years 2001–2004 and 2006–2007. Years 2009 and 2010 were assumed as undisturbed control years, representing ozone variations observed in a single year. Hence, the daily mean of OC $Q_{S,\Delta T}(t_J)$ determined at station S for day of the year t_J was computed by averaging all the corresponding values $Q'_{S,Y}(t_J)$ recorded on the same day of each year Y pertaining to ΔT. Finally, the mean annual variation of parameter $Q_{S,\Delta T}(t_J)$ was smoothed by applying a running average procedure over a 5-day window, which filters the short-period fluctuations and returns the reference OC time-sequence $\overline{Q}_{S,\Delta T}(t_J)$. As an example, Fig. 2 shows these parameters obtained for the data-set collected at Norrköping ($S8$). The values of $Q_{8,2011}(t_J)$ clearly exhibit a sharp decrease of OC in March 2011 with respect to the corresponding values of $\overline{Q}_{8,\Delta T}(t_J)$. Thus, the ratio

$$R_{S,Y}(t_J) = \frac{Q_{S,Y}(t_J)}{\overline{Q}_{S,\Delta T}(t_J)}, \tag{1}$$

provides a measure of the mean relative ozone variations observed throughout the year, Y, at a station, S, with respect to the mean variations determined over the period, ΔT, at the same station. Because of the short observational period at the northernmost station, Ny-Ålesund ($S1$), the period $\Delta T_1=$ [2008–2010] replaced ΔT for the SAOZ data-set and the ratio $R_{1,2011/2010}(t_J) = Q_{1,2011}(t_J)/Q_{1,2010}(t_J)$ was determined to evaluate the 2011 ozone variations registered by UV-RAD.

3.2. Latitudinal features of ozone column variations

The upper panels of Fig. 3 exhibit the OC behaviour at Ny-Ålesund ($S1$) represented in terms of ratios $R_{1,2007}(t_J)$, $R_{1,2011}(t_J)$ and $R_{1,2011/2010}(t_J)$, respectively, while the lower part presents the variations of ratios $R_{S,2005}(t_J)$, $R_{S,2009}(t_J)$, $R_{S,2010}(t_J)$ and $R_{S,2011}(t_J)$ computed for the other 10 stations (Fig. 1). The results obtained at Ny-Ålesund ($S1$) show that at the end of March 2011 OC was about 40% lower than in the reference years and it returned to its common values a few days after that. Similarly, pronounced minima of ratio $R_{S,2011}(t_J)$ were also observed at Scoresbysund ($S2$) and Sodankylä ($S4$), which were both more marked than the ozone variations over the control years in the same season. Moving southwards, the 2011 minima become less pronounced but are still easily recognisable, exceeding in most cases the trends of ratios $R_{S,2009}(t_J)$ and $R_{S,2010}(t_J)$ over the period from late March to late April 2011, and showing a drop of about 25% at 60°N, nearly 20% at 52°N and 15%–18% at 40°–50°N. Fig. 3 shows that the 2011 ozone minima occurred with a lag of several days at the lower-latitude stations and, at the same time, the duration of low ozone episodes became gradually longer moving to south. It can be seen that ratio $R_{S,2005}(t_J)$ also showed deep minima at northern stations due to the Arctic ozone depletion that took place in late February and early March 2005. The 2005 minimum at Scoresbysund ($S2$) is deeper than that observed at Sodankylä ($S4$) and this is reflected in the behaviour of the corresponding minima at the stations further south. The 2005 depletion is not so evident in the southernmost stations in Fig. 3, and it is less pronounced in the easternmost sites.

Such results lead to hypothesize a propagation of the 2011 ozone depletion from high to lower latitudes. To reject the accidental coincidence of the ozone reductions occurring at different latitudes, the analysis in the next subsection searches for a cause-effect connection among the variations occurred at polar and mid-latitude regions.

3.3. Relationship between ozone column variations observed at different latitudes

To support the hypothesis of the propagation of the 2011 ozone depletion from high to lower latitudes, each of ratios $R_{2,2005}(t_J)$ and $R_{4,2011}(t_J)$ was compared with any of the corresponding ratios $R_{S,2005}(t_J)$ for $S = 6, 12, 20, 31$, and $R_{S,2011}(t_J)$ for $S = 8, 11, 18, 28$. The scatter-plots, constructed for each of these pairs were characterised by complicated curves, which could be appreciably simplified taking the ratios at the stations S with a time delay of τ_S days and restricting the comparison period to 51 and 54 days for 2005 and 2011, respectively. Cross-correlating each pair of time-series that represent the corresponding ratios, the time lag τ_S has been determined so that the relationship between $R_{2,2005}(t_J)$ and $R_{S,2005}(t_J+\tau_S)$, and between $R_{4,2011}(t_J)$ and $R_{S,2011}(t_J+\tau_S)$ tended to represent almost one-to-one correspondence. Ratio $R_{2,2005}(t_J)$ determined over the period from 28 January (t'_J) to 19 March 2005 was related to ratios $R_{S,2005}(t_J+\tau_S)$ evaluated over the 51-day period starting at time $t'_J+\tau_S$ for each station S, as the left part of Fig. 4 shows. The similar time-interval for $R_{4,2011}(t_J)$ started on 8 March (t''_J) and finished on 30 April 2011. Consequently, $R_{4,2011}(t_J)$ was compared with $R_{S,2011}(t_J+\tau_S)$ assessed over a 54-day period beginning on $t''_J+\tau_S$ (Fig. 4). The time intervals $[t'_J+\tau_S, (t'_J+\tau_S)+51]$ for the 2005 measurements and $[t''_J+\tau_S, (t''_J+\tau_S)+54]$ for those of 2011 are shown in Fig. 3 (vertical dashed lines), while the corresponding time lags τ_S are reported in Fig. 4.

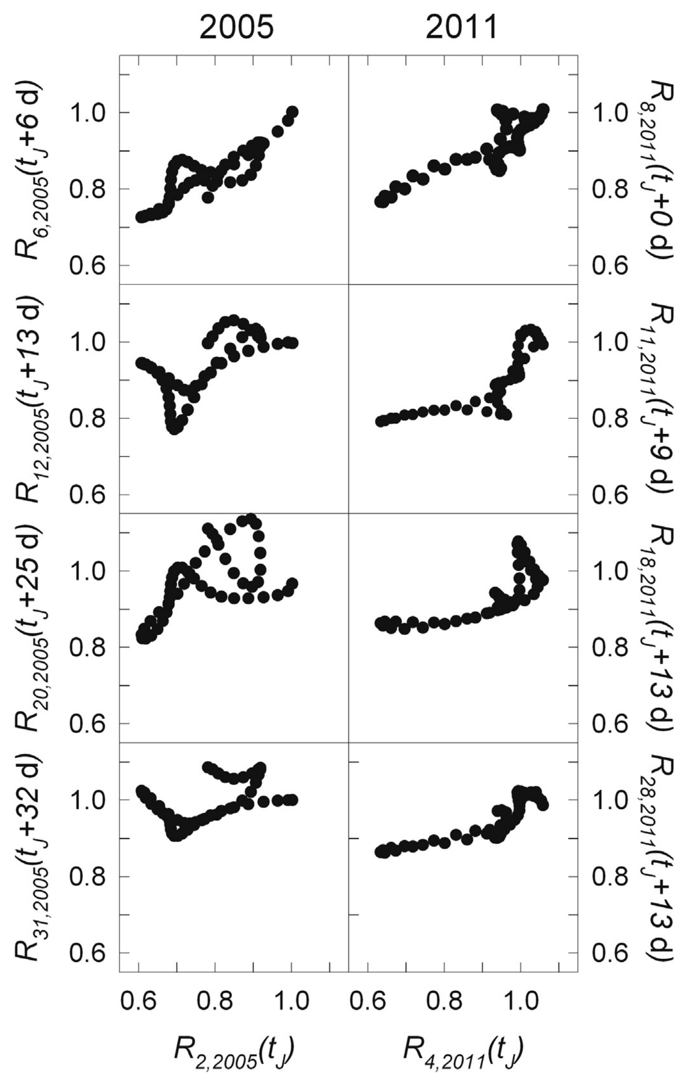

Fig. 4. Left: comparison between each of the ratios $R_{S,2005}(t_J+\tau_S)$ ($S = 6, 12, 20, 31$) and the Scoresbysund ($S2$) ratio $R_{2,2005}(t_J)$. Right: the same for the ratios $R_{S,2011}(t_J+\tau_S)$ ($S = 8, 11, 18, 28$) and the Sodankylä ratio $R_{4,2011}(t_J)$. The time lags τ_S are given in days (d) in the corresponding ordinate legends.

Fig. 4 shows that the relationships between ozone variations at Sodankylä ($S4$) in 2011 and those at each of the four lower-latitude

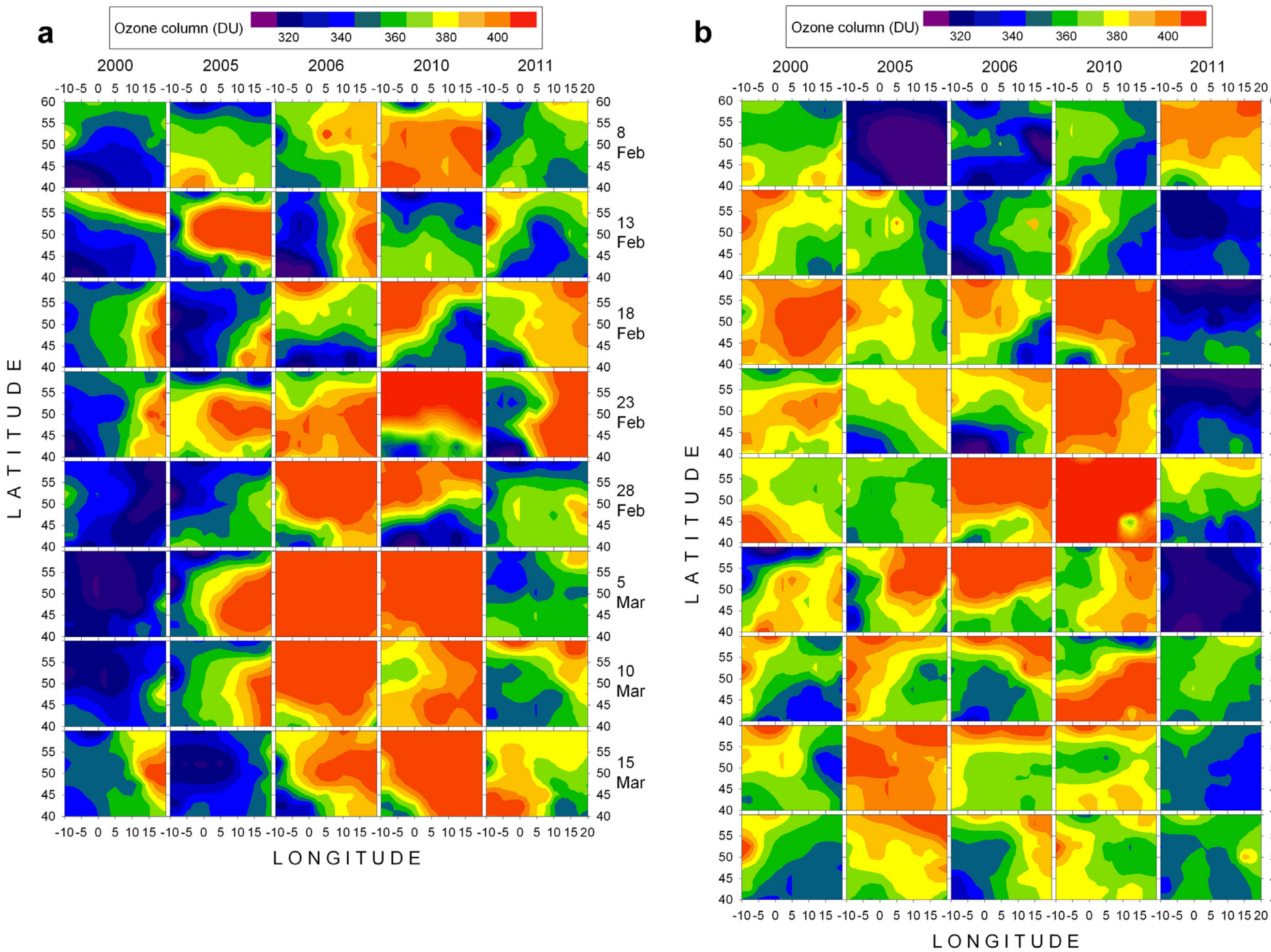

Fig. 5. a. Geographical distributions of daily OC over the selected sector defined in Fig. 1 on different days of the February–March period (indicated on the right side of the graph) and for different years (indicated on the upper side of the graph). The values of OC are given in Dobson Units (DU) and defined by the colour scale reported in the upper part of the graph (the right bound corresponds to OCs ≥ 410 DU). b. As in Fig. 5 a, for the March–April period.

stations closely resemble one-to-one (bijective) maps, i.e. there is a nearly one-to-one correspondence between the OC variations at Sodankylä ($S4$) and those recorded at the four southern stations within the adopted 54-day time-interval. Conversely, the relationships between ratios $R_{2,2005}(t_J)$ and $R_{S,2005}(t_J+\tau_S)$ during the 2005 ozone depletion do not show similar bijective solutions despite various attempts made by varying the parameter t'_J. These results lead to the assumption that nearly one-to-one relationships found for the 2011 data can be considered to arise from a strong cause-effect connections between the corresponding ratios (e.g. Woodward, 2010). However, a similar inference for the ozone variations recorded in spring 2005 cannot be proved on the basis of the ground-based measurements presented here. In addition, unrealistically high values of τ_S found from 2005 data at southern sites render the relationship between high- and mid-latitude ozone variations less reliable. Thus, despite the similarities between the features of ozone depletions observed at Arctic stations in 2005 and 2011, the second one appears to have produced a more pronounced direct effect on OC over a large region, extending its impact to the mid-latitudinal area of the sector under study.

4. Spring-time variability in the ozone column distributions

The distribution of OC over the area between the 10°W and 20°E longitudes and 40°N and 60°N latitudes (Fig. 1) was investigated by analysing the data recorded in February–April 2011, together with (i) the corresponding data collected in 2000 and 2005, both characterised by deep Arctic ozone depletion, and (ii) the 2006 and 2010 data, assumed to present regular OC patterns in the northern polar regions.

Data from ground-based stations were interpolated to obtain the distribution of OC over a grid of 2.5° resolution in both latitude and longitude, covering the sector shown in Fig. 1. Such a procedure allowed us to construct a sequence of OC maps in the Western European area. The interpolation was performed by applying the Shepard (1968) approach, which determines OC $Q_{m,n}(t_J)$ at each grid-point (m,n) placed at latitude m and longitude n, as given by ratio:

$$Q_{m,n}(t_J) = \frac{\sum_{S=1}^{N}\left(d_S^{m,n}\right)^{-2} Q'_S(t_J)}{\sum_{S=1}^{N}\left(d_S^{m,n}\right)^{-2}}, \tag{2}$$

where N is the number of stations considered in the present analysis, $Q'_S(t_J)$ is the daily OC measured at station S and $d_S^{m,n}$ is the mutual distance between the grid-point (m,n) and station S. This distance (in km) was determined by applying the Lambert (1942) formula to the World Geodetic System 1984 spheroid (WGS84, 2000). The data collected at Ny-Ålesund ($S1$) were not considered because of the short observational period, while the stations outside the sector were used to interpolate to the edge of the sector, although including some stations had negligible effect. The results obtained through the adopted interpolation procedure are shown in Fig. 5a and b, as sequences of maps presenting the geographical distributions of daily OC for the period from 8 February to 15 March (Fig. 5a), and from 20 March to 25 April (Fig. 5b) of years 2000, 2005, 2006, 2010 and 2011, respectively, mainly in 5-day steps. It is worth noting that such maps, presenting the OC distribution and reconstructed from the ground-based measurements may become valuable for times when satellite data is unavailable.

Since the polar vortex is the largest factor controlling ozone destruction at high-latitudes, the resulting distributions of OC are related to the behaviour of the vortex during corresponding years. Unlike the Antarctic vortex, the Arctic one is smaller in extent, is warmer and shows a stronger dependence on meteorological conditions, as in the years 2006 and 2010 (see Manney et al., 2011). For that reason the 2006 and 2010 maps have been taken to represent the reference OC distributions characterized by comparatively high values at the northernmost latitudes, due to the dominance of the Brewer-Dobson circulation (WMO, 2010). The extremely cold Arctic vortices formed in the 1999/2000, 2004/2005 and 2010/2011 winters caused a deeper ozone depletion, which perturbed the OC at mid-latitudes, as well (Knudsen and Grooß, 2000; Hauchecorne et al., 2002; Koch et al., 2004; Arnone et al., 2012). The maps presented in Fig. 5a and b show such events. The depletions of 2000 and 2005 started in early February, and the sector was occupied by air masses presenting low ozone amounts from late February to around mid-March in contrast with the same period of the reference 2006 and 2010 years. During the spring of 2011 a similar ozone depletion occurred considerably later starting on the last days of March and lasting until the end of April that could be accounted for specific features of the 2011 vortex behaviour.

Fig. 6a and b present the potential vorticity (PV) for some days from mid February to late April 2005 and 2011 respectively, according to data provided by the European Centre for Medium-Range Weather Forecasts (ECMWF, http://www.ecmwf.int/). The white zones indicate the areas where PV at the 475 K isentropic level exceeded 47 PVU (Potential Vorticity Unit: 1PVU $= 10^{-6}$ K m^2 kg^{-1} s^{-1}) and was considered to outline the

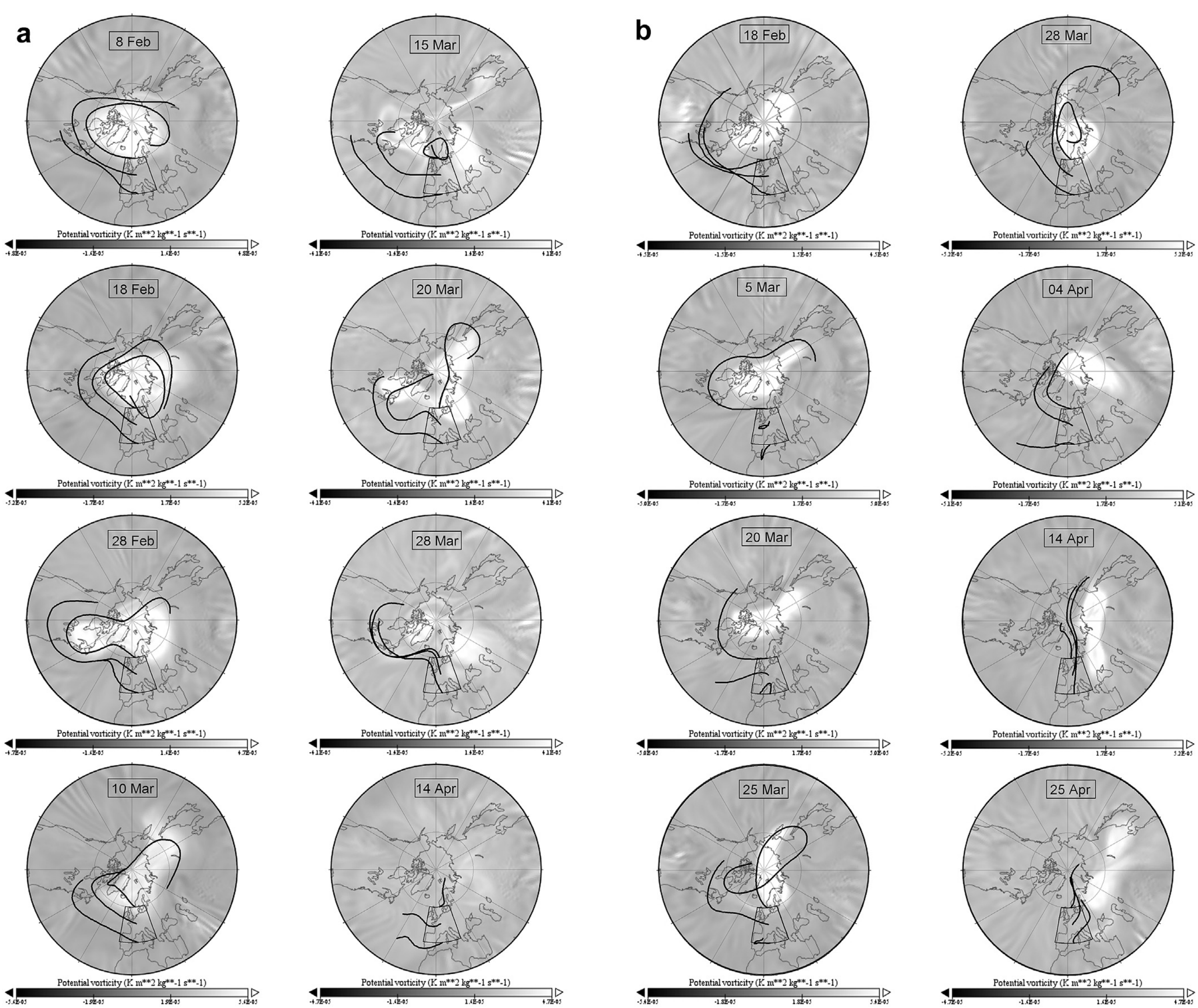

Fig. 6. a. Potential vorticity (PV) over the north hemisphere on some days of 2005 according to ECMWF data. Backward 120-h trajectories evaluated through the HYSPLIT model for 60°N, 50°N and 40°N at the 5°E meridian are also presented by thick black curves, together with the contours of the sector. b. As in Fig. 6a, for 2011.

polar vortex. On the same graphs 120-h backward air parcel trajectories calculated by HYSPLIT model (Draxler and Rolph, 2012) at 20 km altitude for three central points of the sector (60°N, 50°N and 40°N at the 5°E meridian), are also shown. It can be noticed that until 10 March 2005 the transport of air masses to the sector was predominantly from the vortex edge regions, which could explain the low ozone areas that sporadically appeared in the north-west part, as Fig. 5a shows. During the following 10 days of 2005 the break-up processes led to the fragmentation of the vortex. Meantime, the northern area of the sector was affected by both the fragments themselves and the air mass transport from these fragments. Such a scenario is consistent with the ozone distribution presented in Fig. 5a and b. At the end of March 2005 the vortex disappeared (Rösevall et al., 2008) and OC over the sector returned to normal levels. According to Fig. 6b, from mid February to late March 2011 the northernmost borders of the sector were affected by air masses transported from areas near to the vortex edges. Since the 2011 Arctic vortex was anomalously strong (Manney et al., 2011), the exchange with its surroundings was less likely and, hence, these air masses plausibly were not ozone depleted, as Fig. 5a also confirms. At the end of March the vortex changed its shape and the sector tended to be affected by vortex air masses. In the final phase, the vortex tilted off the Pole and moved towards the Euro-Asian region, lasting until late April (Arnone et al., 2012; Kuttippurath et al., 2012). During that period, the sector was affected by the edges of the vortex that could explain the low ozone content exhibited by the maps shown in Fig. 5b.

5. Ozone depletion effects on the surface solar UV irradiance over West Europe

It is well known that the decrease in the atmospheric ozone abundance causes a significant increase in the fraction of solar UV-B irradiance reaching the Earth's surface (from about 295 nm to 315 nm), which can cause relevant damages to the living organisms (Lucas et al., 2006). The 2011 ozone depletion over West Europe took place within a period, when the sun elevation in northern hemisphere rapidly increases that leads to assumption of significant impact on the solar UV radiation at the ground, which is a subject of the analysis in this section.

The sensitivity of the biologically effective UV irradiance at the Earth's surface to the variations of OC is quantified by the Radiation Amplification Factor (RAF), introduced by $I^*/I = (Q/Q^*)^{\mathrm{RAF}}$, where the solar irradiance I is measured (or modelled) for the ozone column Q, while I^* corresponds to Q^* (Madronich, 1993). For the erythemally-weighted irradiance the RAF was evaluated to be about 1.2 for high sun elevations (Seckmeyer et al., 2005). Thus, considering a 40% decrease of OC found in Section 3.2 for the most northerly European sites, the corresponding increase in erythemally weighted UV irradiance is expected to be about 85%. At mid-latitudes, where ozone depletion ranged between 15% and 18%, such an increase was 21%–27%. These percentages show that the polar biosystems were subject to about 4 times higher UV stress than those at mid-latitudes.

Since the erythemal irradiance at high latitudes in the early spring is much lower than that at southern regions, the above percentages could result in different absolute amounts that were assessed through the erythemal dose $D_E[\Delta t, Q_{S,Y}(t_J)]$ calculated as:

$$D_E[\Delta t,\ Q_{S,Y}(t_J)] = \int\limits_{\Delta t} \mathrm{d}t \int\limits_{280\ \mathrm{nm}}^{400\ \mathrm{nm}} A_E(\lambda)\, I[\lambda,\ Q_{S,Y}(t_J)]\,\mathrm{d}\lambda \qquad (3)$$

over a 3-h period Δt symmetrically covering the local noon for each day t_J at any station S presented in the lower part of Fig. 3. $A_E(\lambda)$ is the erythema action spectrum (McKinlay and Diffey, 1987) and the spectral solar irradiance $I[\lambda, Q_{S,Y}(t_J)]$ was calculated for cloudless sky by the Tropospheric Ultraviolet and Visible (TUV) radiative transfer model (Madronich and Flocke, 1997). The following inputs were used: (i) the corresponding OC time-sequences $Q_{S,Y}(t_J)$ and $\overline{Q}_{S,\Delta T}(t_J)$ determined in Section 3.1, (ii) US Subarctic Winter profiles (Anderson et al., 1986) of temperature, ozone and air density for areas above 52°N and the corresponding mid-latitude profiles for areas below 52°N, (iii) surface albedo equal to 0.60 for the sites between 59°N and 70°N, 0.10 for the two sites at 52°N, and 0.04 for the sites below 52°N, and (iv) null aerosol and cloud attenuations (ideal clear-sky conditions). Finally, the parameter $\Delta D_{S,Y}(t_J)$, defined as:

$$\Delta D_{S,Y}(t_J) = D_E[\Delta t,\ Q_{S,Y}(t_J)] - D_E\left[\Delta t,\ \overline{Q}_{S,\Delta T}(t_J)\right], \qquad (4)$$

which is assumed to represent the changes in the erythemal doses arising from the differences between $Q_{S,Y}(t_J)$ and $\overline{Q}_{S,\Delta T}(t_J)$, was calculated. Fig. 7 shows the time-patterns of $\Delta D_{S,Y}(t_J)$, expressed in terms of standard erythemal dose (1 SED = 100 J m^{-2}, Diffey et al., 1997), found for the February–May period of the years $Y = 2005$ and $Y = 2011$.

As can be seen from Fig. 7, the 2005 Arctic ozone depletion event in practice did not produce any significant variations in the erythemal irradiance at latitudes ≥60°N, because it occurred on dates when the sun elevation at noon was very low. The variations of $\Delta D_{S,Y}(t_J)$ below this latitude showed different temporal-patterns for different sites in the March–April period, that makes the relation with the Arctic ozone depletion less likely. The large fluctuations in $\Delta D_{S,Y}(t_J)$ at Norrköping ($S8$), Lindenberg ($S11$)

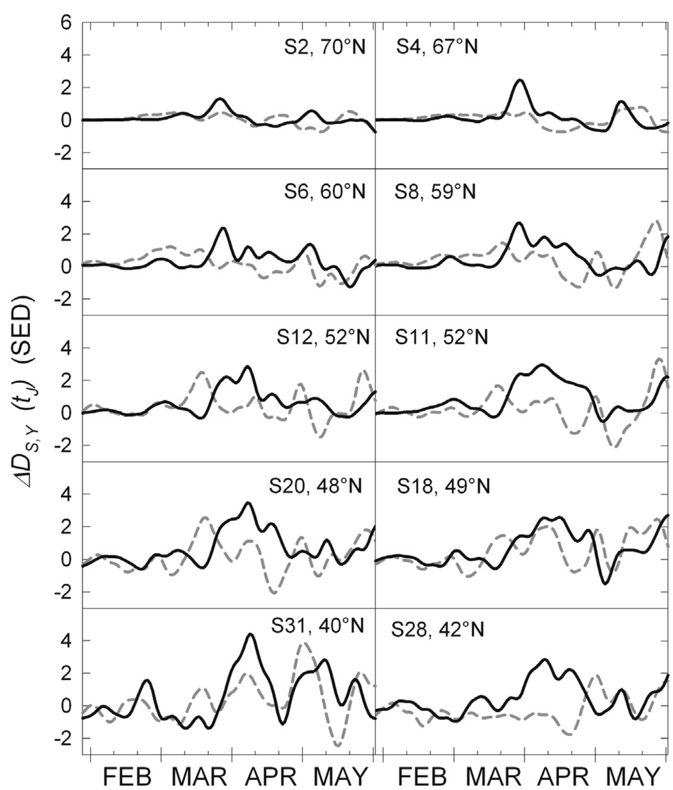

Fig. 7. Variations of the parameter $\Delta D_{S,Y}(t_J)$, expressed in SED (1 SED = 100 J m^{-2}), evaluated in terms of Eq. (4) for the stations represented in the lower part of Fig. 3. The grey dashed curves indicate the corresponding variations found for 2005, while the solid black curves give the 2011 findings.

and Madrid (*S*31) that occurred in May 2005 can be accounted for local ozone changes. In contrast, the echo of the 2011 Arctic ozone loss is clearly seen at both polar and mid-latitude sites. The results highlight another feature: the increase in the absolute value of the erythemal dose at mid-latitudes is almost the same or even higher than that observed in polar areas despite the considerably deeper ozone depletion occurred in the Arctic (see Fig. 3). In fact, while the increase of the erythemal doses at latitudes $\geq 60°$N varied between 1.5 and 2.5 SED, at lower latitudes it ranged from 2.5 to 4.3 SED. Such a discrepancy can be accounted for the solar elevation differences at Arctic and mid-latitudes during the early spring. A similar result was reported by Bernhard et al. (2012) for the UV index.

Hence, the present analysis leads to the conclusion that 2011 Arctic ozone depletion was able to trigger a significant increase in the erythemal dose over Western Europe in April, when the typical climate in the south-west regions is favourable to spend more time outdoors. It is worth pointing out that the above analysis was made for clear-sky conditions to estimate only the ozone effect on the ground-level UV irradiance. The impact of other factors like cloudiness and aerosols (Németh et al., 1996; Seckmeyer et al., 2008), which can modify the present results, is beyond the aim of our investigation. It should be mentioned also that the UV doses were evaluated for a horizontal surface. Bearing in mind the complex geometry of the human body on the one hand and the geometry of the radiation field, on the other, it can be assumed that in some cases the actual exposure might be even higher than that evaluated (Seckmeyer et al., 2013).

6. Conclusions

The response of the mid-latitude ozone column (OC) to the Arctic depletion occurring in the winter-spring period of 2011 was analysed using the ground-based measurements performed at 34 European stations. It was found that OC over Europe was strongly impacted by the phenomenon taking place in the Arctic, which was appreciably more marked than that observed during previous similar events. The significant reduction of the mid-latitude OC started suddenly after the Arctic minimum at late March, and lasted for a rather long period after the ozone recovery in the polar regions. It was estimated that OC over Western Europe decreased by 15%–25% with respect to the mean value determined over the last decade. The distributions of OC were reconstructed for the period from early February to late April for several years between 2000 and 2011. It was found that the 2011 mid-latitude OC was affected by the Arctic depletion later than for other similar occurrences.

The 2011 ozone decrease over West Europe lasted till late April when the solar elevation is considerably higher and, hence, was able to cause an appreciable increase in the erythemal irradiance. The model assessments show that the West Europe inhabitants were affected at noon-time on the clear-sky days of April 2011 by erythemal doses higher by about 3–4 SED than usual. The UV stress suffered by polar biosystems of the North hemisphere was evaluated to be about 4 times higher than that at mid-latitudes.

Analysing the ozone observations performed until now and using model evaluations taking into account the evolution of the ozone depleting substances (ODSs) in the atmosphere, the WMO (2010) assessment determined the two decades up to 2010 as an onset stage of ozone increase. The ozone depletion examined here, which occurred at the end of this stage, suggests that we should be more cautious with premature decisions regarding UV monitoring programs, since similar occurrences cannot be excluded in the following decades until the ODSs have been removed from the stratosphere.

Acknowledgements

The authors gratefully acknowledge the World Ozone and Ultraviolet Radiation Data Centre (WOUDC) for providing the data-set of ground-based measured ozone column, and all organisations responsible for each of the stations used here (WOUDC, 2012; SAOZ, 2012), which afford their data to WOUDC, making this study possible. The European Centre for Medium-Range Weather Forecasts (ECMWF) is also acknowledged for providing the potential vorticity data and the NOAA Air Resources Laboratory (ARL), as well for the provision of the HYSPLIT transport and dispersion model and READY website (http://ready.arl.noaa.gov) used in this publication. The authors thank Prof. Alkiviadis F. Bais (Physics Dept. at Aristotle University, Thessaloniki, Greece) for the discussion and useful comments. This research was developed as a part of the RiS 3305 Project “Ultraviolet Irradiance Variability in Arctic”.

References

Anderson, G.P., Clough, S.A., Kneizys, F.X., Chetwynd, J.H., Shettle, E.P., 1986. AFGL atmospheric constituent profiles (0–120 km). Environ. Res. Pap. 954. Opt. Phys. Div., Air Force Geophys. Lab., Hanscom Air Force Base, Mass.
Antón, M., Bortoli, D., Kulkarni, P.S., Costa, M.J., Domingues, A.F., Loyola, D., Silva, A.M., Alados-Arboledas, L., 2011. Long-term trends of total ozone column over the Iberian Peninsula for the period 1979–2008. Atmos. Environ. 45, 6283–6290.
Arnone, E., Castelli, E., Papandrea, E., Carlotti, M., Dinelli, B.M., 2012. Extreme ozone depletion in the 2010–2011 Arctic winter stratosphere as observed by MIPAS/ENVISAT using a 2-D tomographic approach. Atmos. Chem. Phys. 12, 9149–9165.
Balis, D., Kroon, M., Koukouli, M.E., Brinksma, E.J., Labow, G., Veefkind, J.P., McPeters, R.D., 2007. Validation of Ozone Monitoring Instrument total ozone column measurements using Brewer and Dobson spectrophotometer ground-based observations. J. Geophys. Res. 112, D24S46.
Bernhard, G., et al., 2012. Ozone and UV radiation. Spec. Suppl. Bull. Am. Meteorol. Soc. 93, 129–132.
Brasseur, G.P., Solomon, S., 2005. Aeronomy of the Middle Atmosphere. Springer, pp. 443–531.
Crutzen, P.J., Arnold, F., 1986. Nitric acid cloud formation in the cold Antarctic stratosphere: a major cause for the springtime ‘ozone hole’. Nature 324, 651–655.
Diffey, B.L., Jansen, C.T., Urbach, F., Wulf, H.C., 1997. The standard erythema dose: a new photobiological concept. Photodermatol. Photoimmunol. Photomed. 13, 64–66.
Dobson, G.M.B., Harrison, D.N., Lawrence, L., 1929. Measurements of the amount of the ozone in the Earth’s atmosphere and its relation to other geophysical conditions. Proc. R. Soc. Lond. Ser. A 110, 660–693.
Draxler, R.R., Rolph, G.D., 2012. HYSPLIT (HYbrid Single-particle Lagrangian Integrated Trajectory) Model Access via NOAA ARL READY. NOAA Air Resources Laboratory, Silver Spring, MD. Website. http://ready.arl.noaa.gov/HYSPLIT.php.
Farman, J.C., Gardiner, B.G., Shanklin, J.D., 1985. Large losses of total ozone in Antarctica reveal seasonal $C1O_x/NO_x$ interaction. Nature 315, 207–210.
Fioletov, et al., 2008. Performance of the ground-based total ozone network assessed using satellite data. J. Geophys. Res. 113, D14313.
Flury, T., Hocke, K., Haefele, A., Kämpfer, N., Lehmann, R., 2009. Ozone depletion, water vapor increase, and PSC generation at midlatitudes by the 2008 major stratospheric warming. J. Geophys. Res. 114, D18302,. http://dx.doi.org/10.1029/2009JD011940.
Hauchecorne, A., Godin, S., Marchand, M., Hesse, B., Souprayen, C., 2002. Quantification of the transport of chemical constituents from the polar vortex to midlatitudes in the lower stratosphere using the high-resolution advection model MIMOSA and effective diffusivity. J. Geophys. Res. 107 (D20), 8289. http://dx.doi.org/10.1029/2001JD000491.
Hendrick, F., et al., 2011. NDACC/SAOZ UV–visible total ozone measurements: improved retrieval and comparison with correlative ground-based and satellite observations. Atmos. Chem. Phys. 11, 5975–5995.
Ialongo, Casale, G.R., Siani, A.M., 2008. Comparison of total ozone and erythemal UV data from OMI with ground-based measurements at Rome station. Atmos. Chem. Phys. 8, 3283–3289.
Knudsen, B.M., Grooß, J.-U., 2000. Northern midlatitude stratospheric ozone dilution in spring modeled with simulated mixing. J. Geophys. Res. 105, 6885–6890.
Koch, G., Wernli, H., Buss, S., Staehelin, J., Peter, T., Liniger, M.A., Meilinger, S., 2004. Quantification of the impact in mid-latitudes of chemical ozone depletion in the 1999/2000 Arctic polar vortex prior to the vortex breakup. Atmos. Chem. Phys. Discus. 4, 1911–1940.
Kuttippurath, J., Godin-Beekmann, S., Lefèvre, F., Nikulin, G., Santee, M.L., Froidevaux, L., 2012. Record-breaking ozone loss in the Arctic winter 2010/2011: comparison with 1996/1997. Atmos. Chem. Phys. 12, 7073–7085.

Lambert, W.D., 1942. The distance between two widely separated points on the Earth surface. J. Wash. Acad. Sci. 32, 125–130.
Lucas, R., McMichael, T., Smith, W., Armstrong, B., 2006. Solar ultraviolet radiation: global burden of disease from solar ultraviolet radiation. In: Prüss-Üstün, A., et al. (Eds.), Environmental Burden of Disease Series, No. 13. World Health Organization, Public Health and the Environment, Geneva.
Madronich, S., 1993. UV radiation in the natural and perturbed atmosphere. In: Tevini, M. (Ed.), Environmental Effects of UV (Ultraviolet) Radiation. Lewis, Boca Raton, Florida, USA.
Madronich, S., Flocke, S., 1997. Theoretical estimation of biologically effective UV radiation at the Earth's surface. In: Zerefos, C. (Ed.), Solar Ultraviolet Radiation – Modeling, Measurements and Effects, NATO ASI Series, vol. I52Springer-Verlag, Berlin.
Mangold, A., Grooß, J.-U., De Backer, H., Kirner, O., Ruhnke, R., Müller, R., 2009. A model study of the January 2006 low total ozone episode over Western Europe and comparison with ozone sonde data. Atmos. Chem. Phys. 9, 6429–6451.
Manney, G.L., et al., 2011. Unprecedented Arctic ozone loss in 2011. Nature 478, 469–475.
McKinlay, A.F., Diffey, B.L., 1987. A reference action spectrum for ultraviolet induced erythema in human skin. CIE J. 6, 17–22.
Molina, M.J., Rowland, F.S., 1974. Stratospheric sink for chlorofluoromethanes: chlorine atom catalysed destruction of ozone. Nature 249, 810–814.
Németh, P., Tóth, Z., Nagy, Z., 1996. Effect of weather conditions on UV-B radiation reaching the Earth's surface. J. Photochem. Photobiol. B Biol. 32, 177–181.
Petkov, B., Vitale, V., Gröbner, J., Hülsen, G., De Simone, S., Gallo, V., Tomasi, C., Busetto, M., Barth, V.L., Lanconelli, C., Mazzola, M., 2012. Short-term variations in surface UV-B irradiance and total ozone column at Ny-Ålesund during the QAARC campaign. Atmos. Res. 108, 9–18.
Petkov, B., Vitale, V., Tomasi, C., Mazzola, M., Lanconelli, C., Lupi, A., Busetto, M., 2013. Variations in total ozone column and biologically effective solar UV exposure doses in Bologna, Italy during the period 2005–2010. Int. J. Biometeorol. http://dx.doi.org/10.1007/s00484-012-0621-z (in press).
Pommereau, J.-P., Goutail, F., 1988. O_3 and NO_2 ground based measurements by visible spectrometry during Arctic winter and spring 1988. Geophys. Res. Lett. 15, 891–894.
Rex, M., von der Gathen, P., 2007. Match campaigns to measure stratospheric ozone loss – a key contribution to International Polar Year 2007–2008. WMO Bull. 56 (4), 257–262.
Rösevall, J.D., Murtagh, D.P., Urban, J., Feng, W., Eriksson, P., Brohede, S., 2008. A study of ozone depletion in the 2004/2005 Arctic winter based on data from Odin/SMR and Aura/MLS. J. Geophys. Res. 113, D13301. http://dx.doi.org/10.1029/2007JD009560.
SAOZ, 2012. Système d'Analyse par Observation Zénithale. Retrieved March, 2012, from: http://saoz.obs.uvsq.fr/.
Seckmeyer, G., Bais, A., Bernhard, G., Blumthaler, M., Booth, C.R., Lantz, K., McKenzie, R.L., 2005. Instruments to Measure Solar Ultraviolet Radiation, Part 2: Broadband Instruments Measuring Erythemally Weighted Solar Irradiance. WMO-GAW Report No.164.
Seckmeyer, G., et al., 2008. Variability of UV irradiance in Europe. Photochem. Photobiol. 84, 172–179.
Seckmeyer, G., Schrempf, M., Wieczorek, A., Riechelmann, S., Graw, K., Seckmeyer, S., Zankl, M., 2013. A novel method to calculate solar UV exposure relevant to Vitamin D production in humans. Photochem. Photobiol. 89, 974–983.
Shepard, D.A., 1968. A two-dimensional interpolation function for irregularly-spaced data. In: Proceedings of 1968 23rd ACM National Conference, New York, USA, pp. 517–524.
Siani, A.M., Casale, G.R., Galliani, A., 2002. An investigation on a low ozone episodes at the end of November 2000 and its effect on ultraviolet radiation. Optic. Eng. 41, 3082–3089.
Thompson, A.M., Oltmans, S.J., Tarasick, D.W., von der Gathen, P., Smit, H.G.J., Witte, J.C., 2011. Strategic ozone sounding networks: review of design and accomplishments. Atmos. Environ. 45, 2145–2163.
von der Gathen, P., et al., 1995. Observational evidence for chemical ozone depletion over the Arctic in winter 1991–92. Nature 375, 131–134.
Von Hobe, M., et al., 2006. Severe ozone depletion in the cold Arctic winter 2004–05. Geophys. Res. Lett. 33, L17815.
Werner, R., Valev, D., Atanassov, A., Kostadinov, I., Petkov, B., Giovanelli, G., Stebel, K., Petritoli, A., Palazzi, E., Gausa, M., Markova, T., 2009. Ozone minihole observation over the Balkan Peninsula in March 2005. Adv. Space Res. 43, 195–200.
WGS84, 2000. World Geodetic System 1984. Department of Defense, National Imagery and Mapping Agency. Technical Report TR8350.
WMO, 1998. Scientific Assessment of Ozone Depletion: 1998. World Meteorological Organization Report No. 44. World Meteorological Organization, Geneva.
WMO, 2007. Scientific Assessment of Ozone Depletion: 2006. World Meteorological Organization Report No. 50. World Meteorological Organization, Geneva.
WMO, 2010. Scientific Assessment of Ozone Depletion: 2010. World Meteorological Organization Report No. 52. World Meteorological Organization, Geneva.
Woodward, J., 2010. Causation in biology: stability, specificity, and the choice of levels of explanation. Biol. Phil. 25, 287–318.
WOUDC, 2012. World Ozone and Ultraviolet Radiation Data Centre. In: Data: CNRS, MGO, SMHI, UKMO, U_Oslo, LHMS, U_Manchester, DWD-MOL, KNMI, ME, RMIB, CHMI-HK, MLCD-LU, SHMI, DWD-MOHp, HMS, ASM-ARG, MeteoSwiss, ARPA-VDA, NOAA-CMDL, INME-LC, U_Rome, INME-ZA, AUTH, INME, INME-MU, U_Athens, INTA. Retrieved March, 2012, from: http://www.woudc.org.
Zerefos, C.S., Tourpali, K., Eleftheratos, K., Kazadzis, S., Meleti, C., Feister, U., Koskela, T., Heikkilä, A., 2012. Evidence of a possible turning point in solar UV-B over Canada, Europe and Japan. Atmos. Chem. Phys. 12, 2469–2477.